A Realistic Dynamic Cardiac Phantom for Evaluating Radionuclide Ventriculography: Description and Initial Studies with the Left Ventricular Chamber

Theodore R. Simon, Brandy S. Walker, Sharon Matthiesen, Charles Miller, Jeffrey G. Triebel, J. Edward Dowdey, and Thomas C. Smitherman

Departments of Radiology and Internal Medicine, University of Texas Southwestern Medical Center and the Nuclear Medicine Service, Veterans Administration Medical Center, Dallas, Texas

A phantom was devised to validate scintigraphically determined left ventricular ejection fractions (LVEFs) and cardiac chamber volumes in the following simulated cardiac situations: normal contraction, moderately impaired left ventricular contraction, severely impaired left ventricular contraction, mitral regurgitation, and cardiomyopathy. The phantom, assembled from anatomically realistic cardiac chambers, simulated contraction and expansion using individual chamber pumps coordinated by a microcomputer. Scintigraphic studies were performed by sequential imaging of [^{99m}Tc]pertechnetate introduced into each chamber. The images were analyzed like conventional clinical studies, using both automatic and manual techniques. Scintigraphic techniques correlated with chamber volumes that were determined by weight to yield the following regression formulae: LVEF (by automatic method 1) = 1.08 x LVEF (by weight) −5.11; LVEF (by automatic method 2) = 1.00 x LVEF (by weight) −3.15; and LVEF (by manual method) = 1.04 x LVEF (by weight) −5.08 ml (Correlation coefficients > 0.98). The absolute left ventricular volumes (LVVs), determined by scintigraphy, correlated well with LVVs determined by weight. These correlations were performed with separations between the center of the left ventricle and the collimator varying from 5 cm to 9 cm. The regression formulae for 5, 7, and 9 cm distances were: LVV (by counts) = 0.99 × LVV (by weight) + 0.13, LVV (by counts) = 1.04 × LVV (by weight) + 9.08, LVV (by counts) = 0.88 × LVV (by weight) + 15.25, respectively. At 9 cm, slight volumetric underestimation occurred, as predicted from the work of Fearnow et al., possibly because of oversubtraction of background. Thus, this phantom provides a useful tool for validating scintigraphic cardiac blood-pool studies simulating a wide range of clinically relevant situations.

J Nucl Med 30:542–547, 1989

Substantial problems still complicate accurate measurements of left ventricular contractility and volumes. Since the beginning of this century, radiographic methods for determining cardiac chamber volumes have progressed in tandem with technical developments such as rapid sequence angiography (*1*). The ideal method, however, is not yet available. Calculations of left ventricular volumes by contrast angiocardiography (contrast left ventriculography) require assumptions based upon an appropriate geometric reference solid (*2–8*). Gated blood-pool radionuclide ventriculography (GBP) is currently widely employed as a technique for measuring the left ventricular ejection fraction (LVEF). This ratio of stroke volume to end-diastolic volume provides an estimate of left ventricular contractility. GBP is also widely used as a method for estimating the absolute left ventricular volume (LVV). GBP, which is based on counts rather than on morphologic assumptions, has theoretic advantages over contrast left ventriculography for estimating LVVs. This difference is especially important for cardiac disorders that distort the left ventricular shape.

Received June 3, 1988; revision accepted Dec. 23, 1988.

For reprints contact: Theodore R. Simon, MD, Nuclear Medicine Dept., Building 10, Rm. 1C401, National Institutes of Health, 9000 Rockville Pike, Bethesda, MD 20892.

Previously, radio-opaque solids as well as left ventricular models and casts have served as primary reference standards to validate contrast ventriculographic methods, which in turn have generally served as the secondary reference standards for GBP. However, the limitations of contrast left ventriculography as a reference standard have prompted the search for alternatives. Phantoms of various sorts have been used extensively to study and validate measurements derived from GBP (*9–15*). These phantoms were limited in applicability because they were static, not anatomically realistic in shape, or because they had fewer than four chambers. We have used realistic, expansile phantoms of the individual cardiac chambers in a previous study of self-attenuation (*12*). The principal purpose of the present study was to develop a dynamic cardiac phantom formed by the permanent assembly of such realistic cardiac chamber models to simulate the chambers of the beating heart as each chamber individually responds to control by its own pump. Preliminary investigations using this phantom then addressed its utility to demonstrate changes in LVEF under various simulated clinical conditions and to quantify the LVV at varying distances between the left ventricle (LV) and the camera.

Methods

Hollow, flexible models of both cardiac atria and ventricles were fashioned by the lost wax method, from a commercial plastic model of a normal human heart. Molten wax was poured into each cardiac chamber. A fifth structure, representing the interventricular septum, was sculpted from a wax block. An anatomically correct septum was employed in order to provide realistic separation of the images of the two ventricles and to provide a close representation of attenuation by the septum. These solid wax models were dipped in liquid latex. After hardening, the latex structures served as perma-

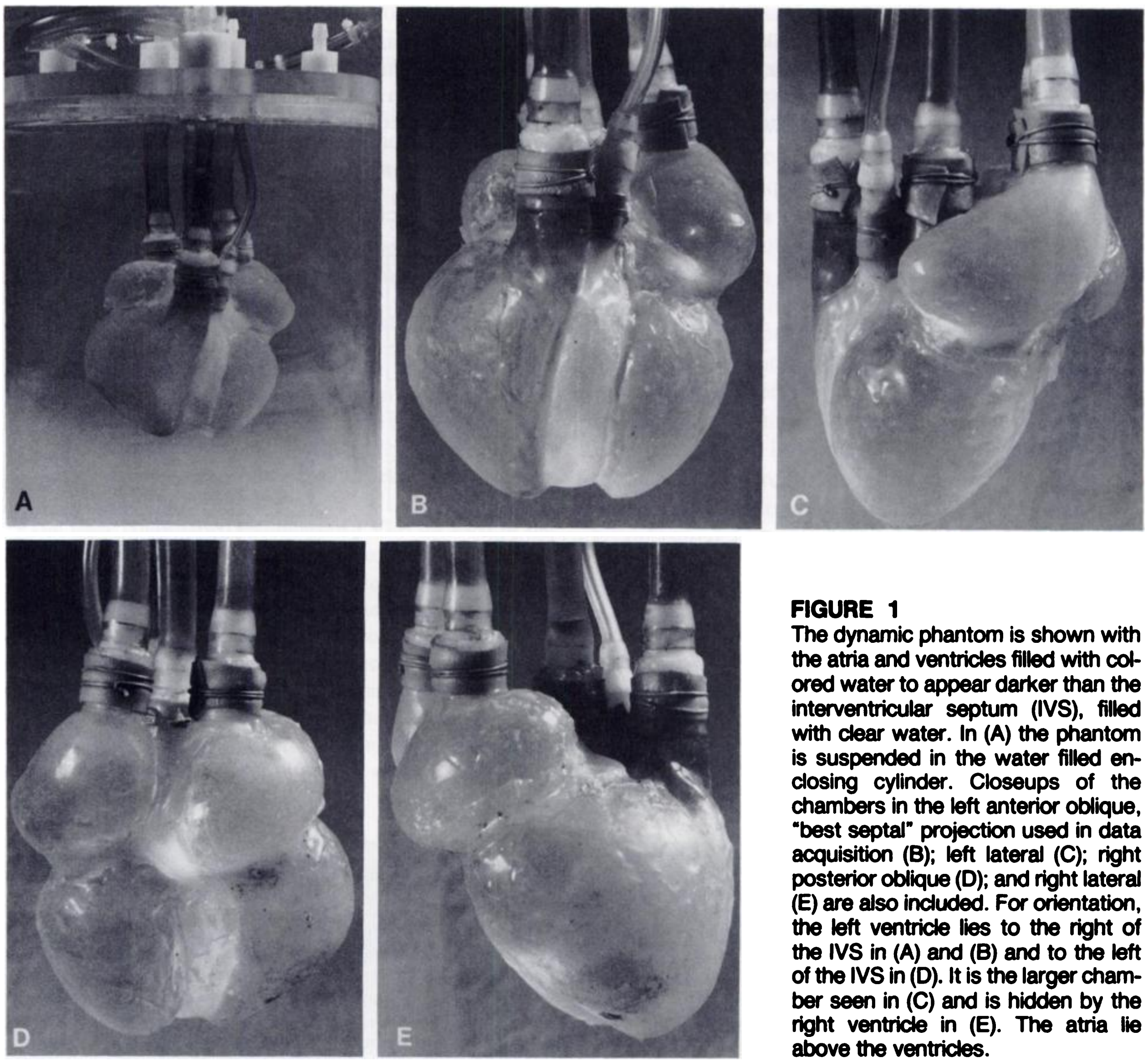

FIGURE 1
The dynamic phantom is shown with the atria and ventricles filled with colored water to appear darker than the interventricular septum (IVS), filled with clear water. In (A) the phantom is suspended in the water filled enclosing cylinder. Closeups of the chambers in the left anterior oblique, "best septal" projection used in data acquisition (B); left lateral (C); right posterior oblique (D); and right lateral (E) are also included. For orientation, the left ventricle lies to the right of the IVS in (A) and (B) and to the left of the IVS in (D). It is the larger chamber seen in (C) and is hidden by the right ventricle in (E). The atria lie above the ventricles.

nent hollow molds. Wax casts of these latex molds were painted with liquid silicone and placed in individual commercial latex condoms after the silicone had cured. The condoms were then painted with a second coat of silicone and the wax was removed. A 12 French polyethylene tube was inserted into each chamber for venting and filling. Each chamber, therefore, was a hollow, three-layered (silicone-latex condom-silicone) expansile model in the shape of a human heart chamber. Small holes that were present or that developed in use were repaired with a few drops of silicone glue. These structures were assembled into their normal anatomic relationships. The resulting cardiac phantom was placed in a cylindrical polyethylene container (18.5 cm inside diameter with 0.5-cm-thick walls) that simulated the noncardiac thoracic structures (Fig. 1). The cylinder was filled with aqueous technetium-99m (^{99m}Tc) pertechnetate having a specific activity of 0.2 mCi/l to simulate thoracic background. The septal chamber was filled with ~ 10 ml of water.

A specifically designed pumping system automatically adjusted the volume of each atrium and ventricle in response to a volume versus time curve constructed using commercial software, Appleplot (Fig. 2). The atrial and the right ventricular curves were derived from classic descriptions by Wiggers (*16*). Moderate and severe left ventricular hypokinesis was adopted from data reviewed by Rackley (*6*). Customized software divided each atrial and ventricular curve into 64 equal time intervals per cardiac cycle. The change in volume for each chamber was converted into directional steps at 0.033 ml per atrial step and 0.0833 ml per ventricular step. The number of steps per interval for each of the four chambers was transmitted to individual stepper motor controllers through customized hardware mounted on an Apple II microcomputer. The controllers instructed each of four stepper motors to power its own cylindrical piston pump, thereby exchanging fluid between the fluid reservoir and the chamber it served. The volume of each chamber at each of the 64 intervals was validated by weight. During imaging, the fluid used within the chambers was aqueous [^{99m}Tc]pertechnetate at a concentration of 2 mCi/l.

Scintigraphic acquisitions simulated the usual protocol for acquiring cardiac gated blood-pool images. A small field-of-view gamma camera [Technicare Sigma 414 interfaced to an image processing computer (MDS A^2 or Siemens Microdelta)] was aimed at an angle to the phantom that provided the best separation of the left and right ventricles, imitating the left anterior oblique "best septal" view used in the clinical situation. The camera was positioned so that it contacted the surface of the cylinder representing the thorax. Low-energy, general all purpose collimation was used with a 15% window centered on the 140 keV ^{99m}Tc peak. A series of 24 images at 22 sec per image was acquired as the phantom moved through its 528-sec simulated cardiac cycle. Each image contained ~ 100,000 counts, a total of ~ 2.4 million counts per sequence. The distance between the center of the left ventricular cham-

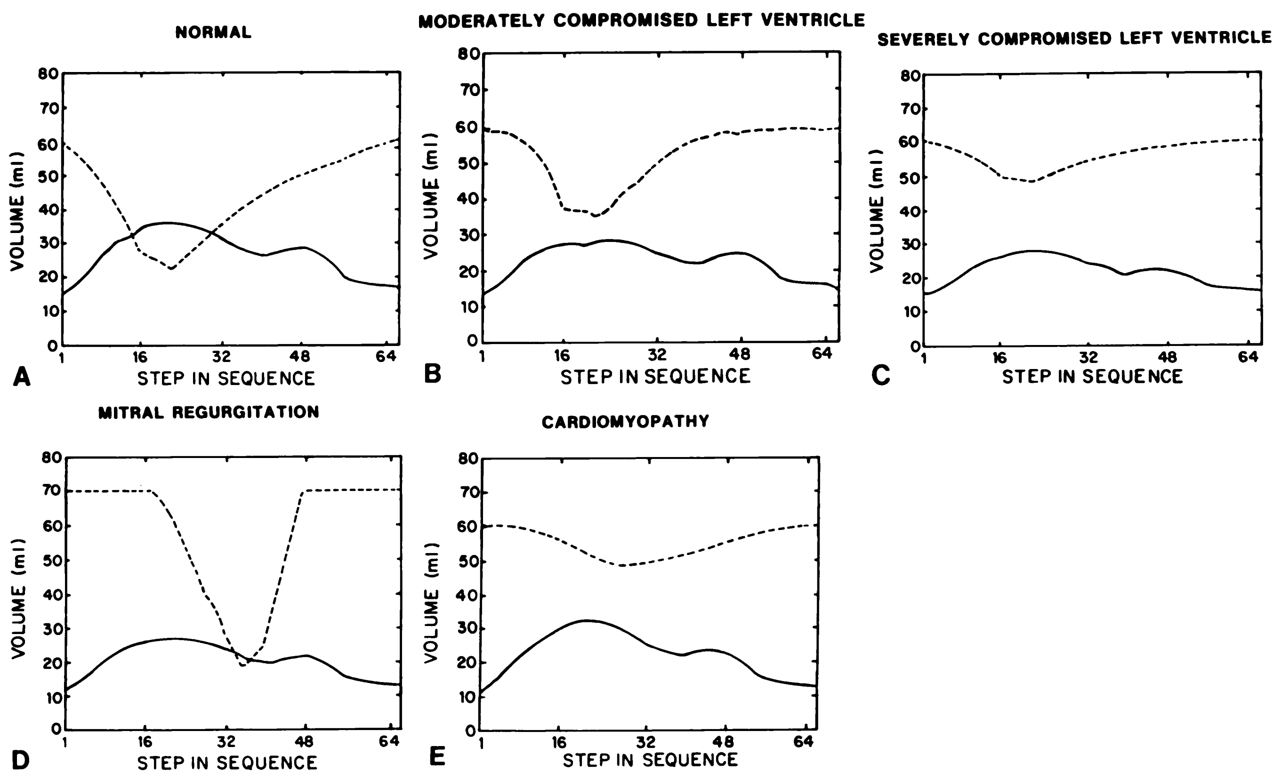

FIGURE 2
Volume versus time curves used to control ventricular and atrial volumes in the cases tested. (A) The normal right ventricular curve used throughout the study. This curve was also used for the normal left ventricular curve. (B) The curve of a moderately impaired left ventricle. (C) The curve of a severely impaired left ventricle. (D) The curve of a left ventricle with mitral regurgitation. (E) The curve of a left ventricle with cardiomyopathy. The dotted and solid lines connect the 64 points in the volume curves of the ventricle and atrium, respectively.

ber and the face of the collimator was 6.1 cm as determined by direct measurements. In order to calibrate counts for deriving the LVV, two 5-min acquisitions were obtained over a plastic syringe containing 5 ml of the 2 mCi/l aqueous solution of [^{99m}Tc]pertechnetate that filled the cardiac chambers.

The 24 64 × 64 pixel matrices, collected at 24 regular intervals during the 64 frame volume versus time sequence, were inspected visually with an endless loop (cine) display and analyzed with each manufacturer's semiautomatic software for calculating LVEF. In addition, two observers manually calculated the LVEF from these displays by outlining end-diastolic, end-systolic, and background regions of interest (ROIs). A periapical background region of interest was subtracted in all three types of analysis.

The images for LVV determinations were independently analyzed twice by each of two experienced observers. Left ventricular volumes used in this experiment were 50 ml and 100 through 150 ml (in 5-ml increments). LVVs were calculated by taking the counts from the sample of "blood" and correcting for the volume of "blood", radioisotopic decay, background in the thoracic phantom, and attenuation. Attenuation was determined by measuring the distance from the center of the ventricle to the collimator and applying the linear attenuation coefficient (μ) of water for broad-beam conditions [0.13/cm (*10,14*)] using the standard formula:

$$\text{Actual Counts} = \text{Observed Counts} \times e^{-\mu d}$$
where d = distance in cm.

Thus, the methods of volume determinations from the scintigrams were practically identical to the technique of Links et al. (*17*) except that we used a value for μ of 0.13/cm instead of 0.15/cm and that we did not identify a deliberately generous left ventricular ROI.

The three count-based estimates of LVEF for each of the five simulated cardiac situations examined were compared to the actual, weight-based, LVEF using linear regression analysis. The count-based absolute LVVs determined for each of the 12 different volumes between 50 ml and 150 ml were also compared to the weight-based actual volumes using linear regression analysis. This comparison was performed for all three distances between the center of the LV and the collimator. The significance of differences among the three regression lines for volume determinations was determined by analysis of variance of the y-intercepts and the slopes of the lines (*18*).

RESULTS

Typical frames from an imaging sequence are illustrated in Figure 3. The images are similar to those obtained during clinical imaging.

The results of the count-based LVEF determinations are outlined in Table 1, along with the values determined by weight. The manually determined values are an average of the readings by the two observers. The intraobserver and interobserver errors were two ejection fraction points based on absolute variation from the mean. The semiautomatic methods varied by less than eight absolute percentage points from the actual values. Except for a single nine-percentage point error, the manual method was within two percentage points of the LVEF based on weight. The s.e.e. determined by the manual technique was smaller, 3.0 ejection fraction percentage points, than those obtained from the semiautomated techniques, which were 4.6 and 5.3. Linear regression analysis of each technique showed a highly linear correlation in each case with the regression formulae closely approaching the lines of identity. The three lines did not significantly differ with respect to slope or y-intercept.

The results from the scintigraphic determinations of LVV are shown in Table 2. At all tested imaging distances, the cardiac phantom within the thoracic phantom demonstrated a highly linear correlation of the measured LVVs to the weight-based volumes. At an imaging distance of 5 cm, the regression formulae hardly differed from the line of identity. At a depth of 7 cm, the relationship was almost as good as that obtained at 5 cm. At 9 cm, however, the scintigraphic technique slightly underestimated volumes. Accordingly, at 9 cm, the slope of the regression line was significantly flatter and the y-intercept significantly higher than at shallower depths.

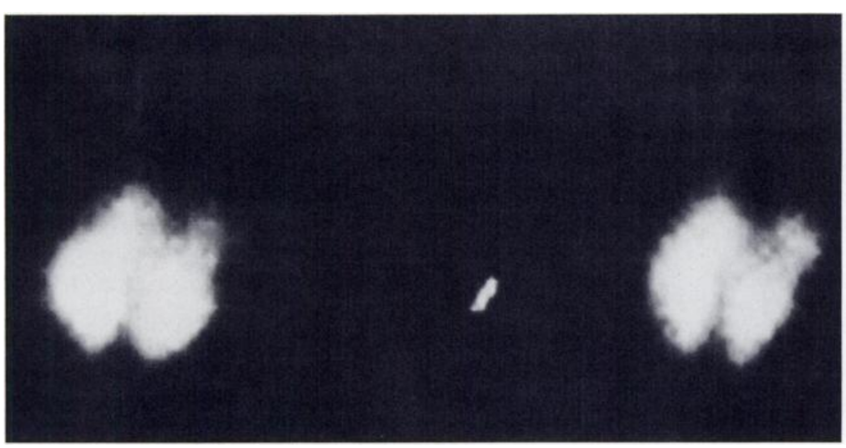

FIGURE 3
Typical frames from a simulated gated blood-pool scintigraphic study of the phantom. The vertical lines are due to activity in the filling tubes. The left image shows ventricular end-diastole; the right, ventricular end-systole.

TABLE 1
Comparison of Weight-Derived Left Ventricular Ejection Fractions to Count-Based Scintigraphic Determinations

Simulated disease	LVEF (Auto 1)	LVEF (Auto 2)	LVEF (Manual)	LVEF (Actual)
Cardiomyopathy	11	22	17	19
Mitral regurgitation	58	55	62	60
Severe global hypokinesis	19	12	18	20
Moderate global hypokinesis	39	36	33	42
Normal	59	63	64	63

Regression formulae, r, s.e.e.
Auto 1 LVEFC* = 1.08 × LVEFA† −5.11, 0.98, 4.61
Auto 2 LVEFC = 1.00 × LVEFA −3.15, 0.99, 5.25
Manual LVEFC = 1.04 × LVEFA −5.08, 0.99, 2.99

* LVEFC = calculated left ventricular ejection fraction, by count-based scintigraphy.
† LVEFA = actual left ventricular ejection fraction, by weight.
r = Pearson's correlation coefficient.

DISCUSSION

The dynamic cardiac phantom described in this study appears to have considerable potential as a standard in assessing the value and limitations of GBP. As such, it is an extension of previous works with cardiac and thoracic phantoms, but it has several important advantages over previously described simpler and static phantoms: it has four chambers and an interventricular septum with realistic shapes and relationships to each other; and the chambers are expandable so that the volume of the chambers with respect to time can be individually altered to provide realistic facsimiles of chamber sizes throughout the cardiac cycle. Phantoms of different sizes can be constructed to mimic cardiac size and function in health and a variety of cardiac disorders. It was designed to determine GBP chamber volumes from as many as 64 frames per cardiac cycle. Evaluation of a radionuclide-filled chamber adjacent to similarly filled chambers of the appropriate sizes, shapes, and positions, with multiple frames throughout a cardiac cycle, provides obvious advantages over fixed, single chamber phantoms in studies of chamber delineation and background subtraction. It may also be useful as a standard for evaluating scintigraphic analysis of diastolic function of the heart. The results using this phantom to measure LVEF and absolute volumes under several conditions, provide some initial indications of the potential usefulness of the phantom as a reference standard. It should have even greater usefulness as a standard for future studies of right ventricular ejection fraction and right ventricular volumes. Unlike the left ventricle, which is reasonably represented by an ellipsoid, the right ventricle cannot be accurately represented by any geometrical solid, which makes confirmation of GBP studies of this chamber with contrast angiography much more difficult (*19*).

TABLE 2
Linear Regression of Count-Based Versus Actual Left Ventricular Weights at Varying Depths of the Cardiac Phantom in the Thoracic Phantom

Distance	Regression formula	*r*	s.e.e.
5	LVVC* = 0.99 LVVA† + 0.13	1.00	0.96
7	LVVC = 1.04 LVVA + 9.08	1.00	1.40
9	LVVC = 0.88 LVVA + 15.25	0.99	3.38

* LVVC = calculated left ventricular volume, by count-based scintigraphy.
r = Pearson's correlation coefficient.
† LVVA = actual left ventricular volume, by weight.

We used a linear attenuation coefficient for water of 0.13/cm in the studies reported here, not the narrow beam value of 0.15/cm that has been used frequently, because narrow beam conditions are not present in imaging with a gamma camera (*9,14*). In the clinical setting, we (*20*) and others (*11,21–24*) have shown that the best estimate for a uniform μ for the thorax is 0.11–0.13/cm, not the narrow beam values of 0.15–0.16/cm that have been used often.

The data of the present study provide additional support for the accuracy of LVEF measurements by count-based GBP in a wide variety of cardiac disorders. The values were as accurate for chambers representing abnormal contraction as for the normal state. The accuracy of the manual and the two semiautomated techniques were roughly comparable. There was no statistically significant difference between the linear regression lines determined by the three methods. Both manual and semiautomatic techniques have their proponents. The automated techniques provide a more objective delineation of the chamber under investigation, but do not always exclude areas that are clearly outside the chamber as judged by visual inspection and may select a region for background subtraction that overlies other blood containing structures, such as the aorta or spleen. The major limitation of this dynamic phantom is the constancy and homogeneity of the noncardiac structures, which differ from the heterogenous air/blood/soft-tissue/bone composition of the normal thorax that changes continually throughout the cardiac and ventilatory cycles. The absence of confounding structures such as great vessels, liver, and spleen, and the homogeneity of background counts in the dynamic phantom undoubtedly contributed to the accuracy of all the techniques; but it is likely that they aided the semiautomated methods somewhat more than the manual one.

The results of the present study also provide additional confirmation of the validity of absolute left ventricular chamber volume determinations at depths of 5–7 cm. At deeper depths, our data suggest that left ventricular volumes may be slightly underestimated when calculated by standard methods of background subtraction. These observations from our four-chamber dynamic phantom are in agreement with the studies of Fearnow et al. (*14*). Those investigators, using a single, hollow acrylic sphere filled with aqueous ^{99m}Tc in a elliptical torso phantom, found that calculated spheric volumes decreased as the distance within the torso increased. This effect, ascribed to excessive background subtraction, became more and more important with increasing the depth of the sphere within the torso phantom. The data from our volume studies suggest that the accuracy of LVEF measurements by GBP could be adversely affected at greater depths of the chamber within the chest and with the use of standard background subtraction techniques. Left ventricular end-diastolic volume might be underestimated to a greater degree than end-systolic volume thus leading to an overestimation of LVEF. Inasmuch as we studied LVEF solely at a depth of 6.1 cm, further studies will be required to confirm this suspicion. Other potentially useful applications of this realistic dynamic cardiac phantom that warrant future work include further simple modifications such as attaching a nonexpansile patch to the left ventricle to make this phantom suitable for studying segmental wall motion abnormalities.

ACKNOWLEDGMENTS

The authors thank Mrs. Deatra Childress for help in preparing the manuscript, Dr. L. Maximillian Buja for help in the accurate positioning of the cardiac chambers, and Dr. Kirk M. Lipscomb for helpful advice and criticism.

REFERENCES

1. Chapman C, Baker O, Reynolds J, Bonte F. Use of biplane cinefluorography for measurement of ventricular volume. *Circulation* 1958; 18:1105–1117.
2. Dodge HT, Sandler H, Ballew DW, Lord JD, Jr. The use of biplane angiocardiography for the measurement of left ventricular volume in man. *Am Heart J* 1960; 60:762–776.
3. Arvedsson O. Angiocardiographic determination of left ventricular volume. *Acta Radiol* 1961; 56:321–339.
4. Kennedy JW, Trenholme SE, Kasser IS. Left ventricular volume and mass from single-plane cineangiocardiogram. A comparison of anteroposterior and right anterior oblique methods. *Am Heart J* 1970; 80:343-352.
5. Cohn PF, Gorlin R, Adamas DF, Chahine RA, Vokonas PS, Herman MV. Comparison of biplane and single plane left ventriculograms in patients with coronary artery disease. *Am J Cardiol* 1974; 33:1–6.
6. Rackley CE. Quantitative evaluation of left ventricular function by radiographic techniques. *Circulation* 1976; 54:862–880.
7. Wynne J, Green LH, Mann T, Levin D, Grossman W. Estimation of left ventricular volumes in man from biplane cineangiograms filmed in oblique projections. *Am J Cardiol* 1978; 41:726–732.
8. Lipscomb K. Cardiac dimensional analysis by use of biplane cineradiography: description and validation of method. *Cath Cardiovasc Diag* 1980; 6:451–464.
9. Siegel JA, Maurer AH, Blasius KM, et al. Absolute left ventricular volumes by an iterative build-up factor analysis of gated radionuclide images. *Radiology* 1984; 151:477–481.
10. Schneider RM, Jaszcak RJ, Coleman RE, Cobb FR. Disproportionate effects of regional hypokinesis on radionuclide ejection fraction: compensation using attenuation-corrected ventricular volumes. *J Nucl Med* 1984; 25:747–754.
11. Harris CC, Greer KL, Jaszcak RJ, Floyd CE, Jr, Fearnow EC, Coleman RE. Tc-99m attenuation coefficients in water-filled phantoms determined with gamma cameras. *Am Assoc Phys Med* 1984; 11:681–685.
12. Simon TR, Dowdey JE, Lipscomb KM, Smitherman TC. Correlation of scintigraphy and angiography for ventricular volume determinations using realistic cardiac phantoms: the unimportance of self-attenuation. *Radiology* 1985; 154:232–233.
13. Siegel JA, Wu RK, Maurer AH. The buildup factor: effect of scatter on absolute volume determination. *J Nucl Med* 1985; 26:390–394.
14. Fearnow EC, III, Stanfield JA, Jaszcak RJ, Harris CC, Coleman RE. Factors affecting ventricular volumes determined by a count-based equilibrium method. *J Nucl Med* 1985; 26:1042–1047.
15. Siegel JA. The effect of source size on the buildup factor calculation of absolute volume. *J Nucl Med* 1985; 26:1319–1322.
16. Wiggers CJ. *Circulatory dynamics*. New York: Grune & Stratton, Inc., 1952.
17. Links JM, Becker LC, Shindledecker JG, et al. Measurement of absolute left ventricular volumes from gated blood pool studies. *Circulation* 1982; 65:82–91.
18. Zar JH. *Biostatistical analysis*. Englewood Cliffs, NJ: Prentice-Hall. 1974:198–235.
19. Reedy T, Chapman CB. Measurement of right ventricular volume by cineangiofluorography. *Am Heart J* 1963; 66:221–228.
20. Keller AM, Simon TR, Smitherman TC, et al. Direct determination of the attenuation coefficient for radionuclide volume measurements. *J Nucl Med* 1987; 28:102–107.
21. Fearnow EC, Jaszcak RJ, Harris CC, et al. Esophageal source measurement of Tc-99m attenuation coefficient for use in left ventricular volume determinations. *Radiology* 1985; 157:517–520.
22. Nickoloff EL, Perman WH, Esser PD, et al. Left ventricular volume: physical basis for attenuation corrections in radionuclide determinations. *Radiology* 1984; 152:511–515.
23. Guiteras P, Green M, Desouza M, et al. Count-based scintigraphy method to calculate ventricular volumes in children: in vitro and clinical validation. *JACC* 1985; 5:963–972.
24. Rabinovitch MA, Kalff V, Koral E, et al. Count-based left ventricular volume determination utilizing a left posterior oblique view for attenuation correction. *Radiology* 1984; 150:813–818.